Emission Control

International Edition: DOI: 10.1002/anie.201605397
German Edition: DOI: 10.1002/ange.201605397

The Significance of Lewis Acid Sites for the Selective Catalytic Reduction of Nitric Oxide on Vanadium-Based Catalysts

Adrian Marberger, Davide Ferri, Martin Elsener, and Oliver Kröcher*

Abstract: *The long debated reaction mechanisms of the selective catalytic reduction (SCR) of nitric oxide with ammonia (NH_3) on vanadium-based catalysts rely on the involvement of Brønsted or Lewis acid sites. This issue has been clearly elucidated using a combination of transient perturbations of the catalyst environment with operando time-resolved spectroscopy to obtain unique molecular level insights. Nitric oxide reacts predominantly with NH_3 coordinated to Lewis sites on vanadia on tungsta–titania (V_2O_5-WO_3-TiO_2), while Brønsted sites are not involved in the catalytic cycle. The Lewis site is a mono-oxo vanadyl group that reduces only in the presence of both nitric oxide and NH_3. We were also able to verify the formation of the nitrosamide (NH_2NO) intermediate, which forms in tandem with vanadium reduction, and thus the entire mechanism of SCR. Our experimental approach, demonstrated in the specific case of SCR, promises to progress the understanding of chemical reactions of technological relevance.*

Abatement of harmful NO_x is a major objective of environmental and health protection policies as a result of the increasing emissions from power plants and vehicles in rapidly developing countries. Efficient NO_x removal from exhaust gases of stationary sources is achieved by reacting NH_3 on a solid catalyst, typically consisting of dispersed vanadia on tungsta–titania (V_2O_5-WO_3-TiO_2), according to the standard selective catalytic reduction (SCR) process.[1]

$$4\,NO + 4\,NH_3 + O_2 \rightarrow 4\,N_2 + 6\,H_2O \qquad (1)$$

The increasingly stringent emission regulations in the transport sector also make this technology attractive for controlling the exhaust of mobile sources; especially diesel trucks, railroad diesel engines, and more recently, ship engines. Despite the widespread use of SCR, some molecular aspects of the reaction mechanism remain controversial.[2] The advent of powerful computational resources, the search for catalyst formulations counteracting the implicit drawbacks of vanadium-based catalysts,[3] and the development of low-temperature SCR catalysts for automotive applications, have rejuvenated the debate on the nature of the active center. The mechanistic aspects of SCR using vanadium were summarized by Busca et al.[4] The reaction proceeds according to the stoichiometry of Reaction (1) and the two nitrogen atoms of the N_2 product originate, one each, from NO and NH_3. It is generally accepted that the mechanism comprises an acid site where NH_3 is activated and a redox site that requires oxygen to be regenerated. The Brønsted and Lewis acid sites are responsible for the adsorption of NH_3 and have thus been anticipated to be essential for the reaction mechanism. While Brønsted acid sites bind NH_3 to form NH_4^+ (B_{NH_3}), Lewis acid sites coordinate NH_3 directly with a metal atom (L_{NH_3}). NO reacts on the acid sites according to an Eley–Rideal mechanism, accompanied by the reduction of V^{5+} to V^{4+}. It is also recognized that the role of oxygen is to restore the $V^{5+}O_x$ active center. Various experimental and theoretical studies have tackled the crucial issue of the involvement of either B_{NH_3} or L_{NH_3} sites in the standard SCR reaction without reaching unequivocal conclusions. Ramis et al.[2b] reported a mechanism based on L_{NH_3} active species that encompasses the formation of a NH_2NO reaction intermediate. B_{NH_3} was later proposed by Topsøe[2c] as the active center. Given the large excess of B_{NH_3} species compared to L_{NH_3}, especially with the introduction of tungsta in the catalyst formulation, the SCR activity was correlated with the change of B_{NH_3} coverage.[5] However, two considerations seem to complicate the Brønsted acid mechanism. Ammonia must lose all protons to form the N_2 product, thus making the initial protonation to NH_4^+ an apparently superfluous step. The energy barrier for the reaction involving a Brønsted acid site is also higher than that comprising a Lewis acid site.[6] By comparison, L_{NH_3} is more resistant to desorption at a given temperature[7] and demonstrates higher heat of adsorption than B_{NH_3}.[8] Although the two reaction pathways probably do not exclude each other, it is essential to understand whether either or both species are relevant.

Spectroscopy contributed considerably to the formulation of the proposed reaction mechanisms.[2b–d,9] However, we note that this precious mechanistic information was derived under steady-state conditions, thus under less suitable experimental conditions and inappropriate time scales to observe active and intermediate species and to describe the working catalyst. Moreover, the widely used temperature programmed desorption method can only predict the amount and stability of acid sites, but is intrinsically ambiguous with respect to the nature and reactivity of the acid site(s) directly involved in the reaction. Important mechanistic details were obtained on vanadium-based catalysts also by the transient-response method,[10] but without implementation of spectroscopic measurements. Transient experiments are more suitable to

[*] A. Marberger, Dr. D. Ferri, M. Elsener, Prof. O. Kröcher
Paul Scherrer Institut
5232 Villigen PSI (Switzerland)
E-mail: davide.ferri@psi.ch
A. Marberger, Prof. O. Kröcher
Institute of Chemical Science and Engineering
École polytechnique fédérale de Lausanne (EPFL)
1015 Lausanne (Switzerland)

Supporting information for this article can be found under: http://dx.doi.org/10.1002/anie.201605397.

disclose the nature of active centers on a catalyst surface. From a spectroscopic perspective, second to sub-second time-resolution is required to capture relevant structural changes while the catalytic system is perturbed. To date, little time-resolved examination of this kind has been reported for a state-of-the-art V_2O_5-WO_3-TiO_2 SCR catalyst.

Herein, we describe the use of time-resolved infrared and visible spectroscopy to demonstrate the unambiguous involvement of NH_3 bonded to Lewis acid sites in the SCR mechanism. At low temperature, the B_{NH_3} species barely contribute to the activity of a vanadium-based catalyst and solely L_{NH_3} species participate in the standard SCR reaction. We are also in the position to associate the V^{5+}/V^{4+} redox pair with the Lewis acid site. The striking experimental observations herein provide a new perspective on the mechanism involved (based on Lewis acid sites) that may encourage the use of our experimental approach as a tool to assist the design of SCR catalysts. This holds specifically for vanadium-based catalysts, but because of the general applicability of the method the development of other types of catalysts should profit too.

The selected catalyst for this study comprised 2 wt % V_2O_5 supported on 10 wt % WO_3-TiO_2 (VWT), a commonly used composition for state-of-the-art vanadium-based SCR catalysts.[11] The relatively low vanadium loading guaranteed, on the one hand, sub-monolayer coverage of oxo-species (ca. 25 %), which provided high selectivity and stability, and on the other hand, sufficiently high activity in the SCR reaction for most commercial applications. The NO reduction behavior measured in the spectroscopic cell in the temperature range 150–350 °C was comparable to that obtained in a tubular quartz reactor (Supporting Information, Figure S1), thus ensuring transferability of the spectroscopic data. When examined by diffuse reflectance infrared spectroscopy (DRIFTS), NH_3 adsorption at 250 °C followed by desorption in 5 vol % O_2/N_2 (Figure 1 a) was characterized by the features of ammonium ions (NH_4^+) adsorbed on Brønsted acid sites (B_{NH_3}; 3200–2700, 1670, and 1423 cm^{-1}) and NH_3 coordinated to Lewis acid sites (L_{NH_3}; 3250, 1603, and 1250 cm^{-1}). These features were easily assigned on the basis of existing literature.[2b,12] The coverage of both species was only slightly diminished upon desorption. Various negative peaks were associated with the coordination of NH_3 to titanium and tungsten hydroxy groups, vanadyl (V=O) and tungstenyl (W=O) groups, and residual sulfate (S=O) species. From the perspective of infrared spectroscopy, it is obvious that NH_3 adsorption on Brønsted acid sites was dominant and that tungsta played a major role in this respect.

When residual adsorbed NH_3 (after desorption at 250 °C) was reacted with 500 ppm $NO/O_2/N_2$ while recording DRIFTS spectra at 0.9 s/spectrum, the first evident effect was that these species were consumed before nitrosyl species (NO^+) and water started to populate the surface of the catalyst (Figure 1 a). Only a deeper inspection of the time-resolved spectra demonstrated that the consumption rates of L_{NH_3} and B_{NH_3} were not identical upon exposure to NO. This is best seen from the temporal evolution of the two species and NO^+ (Figure 1 b). Consumption of L_{NH_3} occurred in two stages, which could be distinguished by the time evolution of

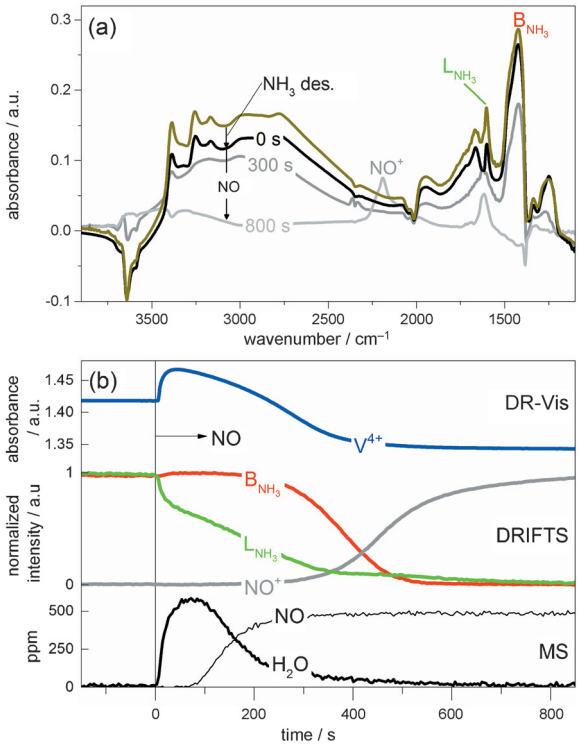

Figure 1. Transient infrared and visible spectra of NO reaction on NH_3-equilibrated V_2O_5-WO_3-TiO_2. a) DRIFT spectra after 500 ppm NH_3 adsorption (15 min), desorption (15 min) followed by NO (500 ppm) addition. b) Temporal evolution of selected signals during addition of NO from identical DRIFT and DR-Vis measurements and from online gas analysis by mass spectrometry. DRIFTS: δ_{as}(N–H) of L_{NH_3}, δ_{as}(N–H) of B_{NH_3}, and ν(NO) of NO^+. DR-Vis: V^{4+} (700 nm, d–d transition). Negative and positive absorbance values indicate consumption and formation of species, respectively. Conditions: O_2/N_2 (5 vol %); 250 °C.

L_{NH_3} rather than by the presence of two distinct spectroscopic signatures. An instantaneous removal of approximately 30 % of L_{NH_3} ($L_{NH_3}(1)$) was followed by a slower consumption of L_{NH_3} ($L_{NH_3}(2)$). Only when L_{NH_3} had been almost completely consumed, did the signal of NO^+ start to intensify. B_{NH_3} coverage at this point was still approximately 70 %. B_{NH_3} only started declining long after reaction of L_{NH_3}. The simultaneous mass spectrometric data undoubtedly demonstrated that the water product of standard SCR evolved parallel to the consumption of L_{NH_3}, thus reflecting the occurrence of the SCR reaction in the early stages of NO admittance. This is further supported by the very similar ratio between consumed NO and evolved water (1.53) relative to the stoichiometry of the standard SCR reaction (1.5).

Exposure to NO also had an immediate impact on the oxidation state of vanadium (Figure 1 b; Supporting Information, Figure S3) in an identical diffuse reflectance visible (DR-Vis) spectroscopy experiment. NO caused a rapid initial reduction, which was monitored using the d–d transition at 700 nm as the fingerprint of V^{4+}.[13] Reduction was followed by a slower re-oxidation before returning to a constant (and on average higher) oxidation state after all adsorbed NH_3 had been consumed. Hence, the time-resolved measurement of

Figure 1 clearly demonstrates that NO reacted primarily with L_{NH_3} and simultaneously enhanced reduction of V^{5+} to V^{4+}, compared to NH_3 adsorption. After the fast initial reaction of NO with L_{NH_3}, the SCR reaction slowed down because of the decreasing L_{NH_3} coverage and the increasing levels of V^{5+}. B_{NH_3} started declining only after consumption of $L_{NH_3}(2)$. Although we cannot exclude that B_{NH_3} converts into L_{NH_3} before reacting, this demonstrates that at low temperature only the Lewis acid sites are SCR active. Moreover, NO is activated on a Lewis acid site occupied by NH_3 in tandem with reduction of V^{5+} to V^{4+}. As long as L_{NH_3} is available, NO cannot adsorb as NO^+ and gradually consumes the remaining NH_3 species.

The rates of initial consumption of L_{NH_3} and of the parallel initial reduction to V^{4+} were independent of temperature (200–250 °C) and presence of oxygen (Figure 2), suggesting that $L_{NH_3}(1)$ is not involved in the rate-determining step. On the contrary, the fraction of $L_{NH_3}(2)$ increased with decreasing temperature, while its consumption rate decreased. $L_{NH_3}(2)$ was susceptible to the absence of oxygen. Admittance of NO in the absence of oxygen (Figure 2c) consumed only $L_{NH_3}(1)$, which reacts faster at all temperatures. However, no further L_{NH_3} consumption was observed once consumption of $L_{NH_3}(1)$ had occurred. This observation suggests that $L_{NH_3}(1)$ does not require gas phase oxygen to complete the SCR reaction.

The absence of oxygen further discards the possibility for NO_2 to be the source of the initial fast decay of L_{NH_3} (fast SCR).[14] When the catalyst was equilibrated with NH_3 in the absence of oxygen after reaction with NO (Figure 2d), no fast L_{NH_3} consumption was detected. This measurement demonstrates decisively that $L_{NH_3}(1)$ does not need oxygen to react but cannot be regenerated if oxygen is absent. Therefore, this active site is an oxidized center. The reaction of $L_{NH_3}(2)$ can instead be associated with the slower re-oxidation that was clearly temperature dependent, in agreement with oxygen being involved in the rate-determining step.[14b] Without oxygen, re-oxidation did not occur and a constant V^{4+} content was obtained over time on stream. This data encourages us to propose the existence of $V^{5+}O_x$ Lewis acid sites that are already arranged in an optimum configuration to react with NO after NH_3 adsorption. The structure of these sites is addressed below.[15] Once these sites have been reduced by the reaction of coordinated NH_3 with NO, they need to be regenerated by oxidation of V^{4+}.

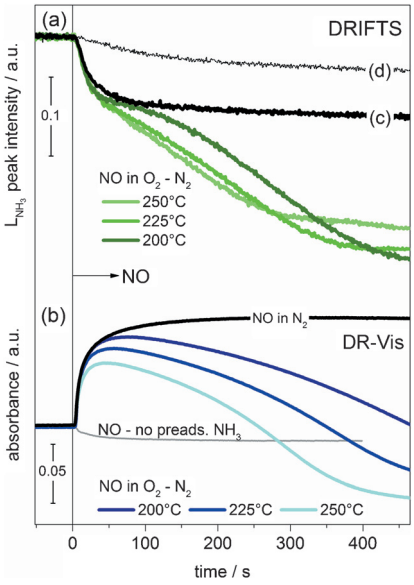

Figure 2. Temperature dependence of NO reaction on NH_3-equilibrated V_2O_5-WO_3-TiO_2. Temporal evolution of selected a) DRIFTS and b) DR-Vis signals during NO addition at 200, 225, and 250 °C (with and without O_2) in identical measurements to that of Figure 1. c) and d) Traces correspond to temporal evolution of L_{NH_3} in two consecutive runs in the absence of oxygen and with NH_3 adsorption/desorption intervals. DRIFTS: $\delta_{as}(N{-}H)$ of L_{NH_3}; DR-Vis: V^{4+} (700 nm).

The significance of L_{NH_3} for SCR was confirmed by an identical measurement, which included water in the feed gas during NH_3 adsorption/desorption and NO admittance (Supporting Information, Figure S5—S7). Water is reported to decrease NO conversion, which we also observed in the DRIFT cell (Supporting Information, Figure S1). As a consequence, the overall levels of both L_{NH_3} and B_{NH_3} before NO dosage were lower in the spectra as a result of competition with water. Nevertheless, the relative temporal evolution of the two species remained identical, suggesting that water decreases the reactivity of VWT by suppressing a fraction of Lewis acid sites available for reaction—in particular $L_{NH_3}(1)$ that was evidently absent.

The experiments described so far undoubtedly demonstrate two crucial steps of the reaction mechanism of standard SCR reaction on a VWT catalyst: 1) the direct involvement of the V^{5+} Lewis acid site, and 2) the rate-determining step, which is the oxidation of V^{4+} by oxygen. This is presented for clarity in Scheme 1 (steps (a) and (d), respectively), within the paradigm of the catalytic cycle proposed by Ramis et al.,[2b] based on Lewis acid sites. We were able to obtain an even more complete picture of the reaction mechanism under more realistic reaction conditions than those of Figure 1 and Figure 2, by periodically perturbing the atmosphere around the catalyst while acquiring time-resolved spectroscopic data. This approach mimics the SCR conditions better than the

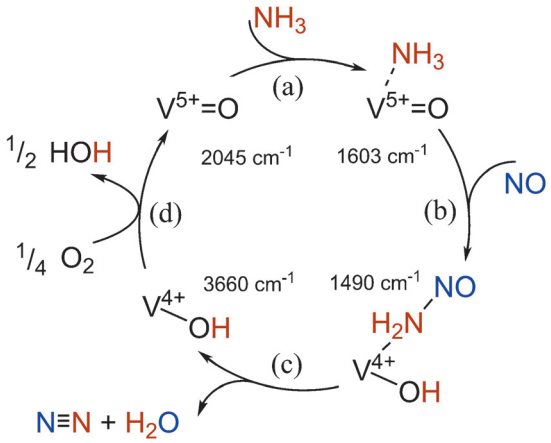

Scheme 1. Reaction mechanism of standard NH_3-SCR.

single transient experiment of Figure 1. The short time-scale inspection of the SCR reaction using modulated excitation spectroscopy[16] can trace the surface changes with additional precision because of phase sensitive analysis.

The most valuable modulation sequence consisted of NO pulses in a continuous flow of NH_3/O_2 (Figure 3d; Supporting Information, Figure S10), that is, on a catalyst surface permanently covered by adsorbed NH_3. Other relevant

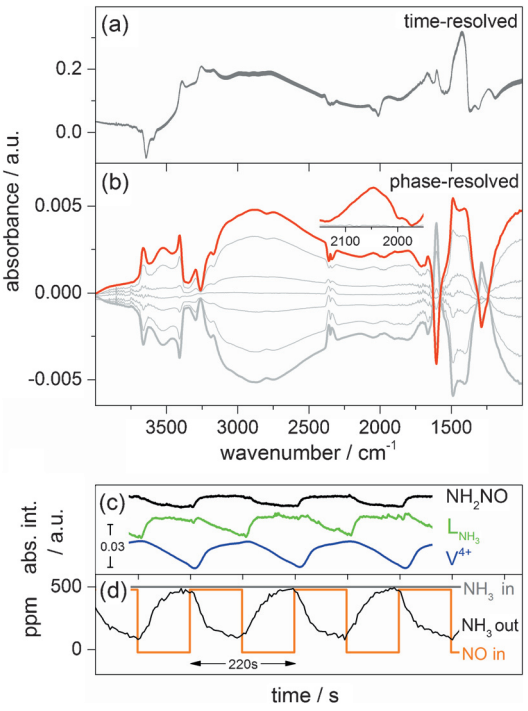

Figure 3. The concentration modulation approach: NO pulses in NH_3. a) Time-resolved DRIFT spectra during a full $NO+NH_3+O_2/NH_3+O_2$ modulation experiment at 250 °C ($T=220$ s). b) The corresponding set of selected phase-resolved data ($\varphi^{PSD}=150$–$320°$); in-phase spectrum (red). c) Temporal evolution of selected signals from the time-resolved DRIFT and DR-Vis spectra over multiple periods. d) Representation of the pulse sequence (NH_3 in, NO in) and experimental FTIR gas analysis (NH_3 out). Conditions: NH_3 (500 ppm), NO (500 ppm), O_2 (5 vol%) in N_2.

sequences for the discussion are presented in Figure 4. Only the phase-resolved spectra were able to reveal subtle but important changes as the SCR reaction was switched on and off repeatedly by NO pulses (Figure 3b). These changes mirrored those observed in the single transient experiment of Figure 1 and were essentially identical in the case of shorter pulses (Supporting Information, Figure S10). Despite their dominant presence in the time-resolved spectra (Figure 3a), none of the changes could be associated with B_{NH_3}, thereby confirming its extraneousness with respect to SCR. On the contrary, L_{NH_3} played a major role in the spectra. It exhibited signals of opposite sign to that of two signals at 1490 and 1400 cm^{-1}, which were otherwise hidden in the time-resolved spectra by the persistent B_{NH_3} signals. These two signals were slightly phase shifted, suggesting that they did not belong to the same species.

The features at 1603 and 1490 cm^{-1} did not reflect NH_3 adsorption/desorption because of their opposite sign. This process was rather mimicked by the sequence in Figure 4j–l, where a minor fraction of B_{NH_3} was also seen to contribute to the phase-resolved spectra and with the same sign as L_{NH_3}. We could assign the signal at 1490 cm^{-1} to the nitrosamide intermediate (NH_2NO, ν(NO); Scheme 1b).[2b] The assignment was confirmed by the temporal evolution of the feature in this sequence and in that obtained by alternating NO and NH_3 pulses. In the NH_3/O_2 pulse (Figure 3c), the replenishment of L_{NH_3} consumed in the previous $NO+NH_3+O_2$ pulse was accompanied by the disappearance of nitrosamide as a result of the absence of NO. This corresponds to interrupting the catalytic cycle at step (b) in Scheme 1. Nitrosamide sharply intensified again when NO was admitted concomitantly to the consumption of L_{NH_3}. Hence, L_{NH_3} reacted repeatedly with NO, as in the experiment of Figure 1, which was confirmed by the loss of gas phase NH_3 (Figure 3d). When NO pulses were alternated with NH_3 pulses (Figure 4d), the SCR reaction occurred only briefly at the valve switch. Consistent with its intermediary nature, nitrosamide was formed rapidly at each pulse before returning to lower levels because the gas composition was either only NO or only NH_3. The need for both NH_3 and NO for V^{5+} reduction was confirmed by the DR-Vis data of this sequence (Figure 4f). The V^{4+} level increased only at the beginning of the $NO+O_2$ pulse, since Lewis acids were covered by NH_3 reacting with NO at the V^{5+} center. V^{4+} slowly re-oxidized in the NO pulse, in response to oxygen and the slight oxidative character of NO (compare with Figure 2b). The change in L_{NH_3} was larger in this sequence because of the continuous addition and removal of gas phase NH_3 and was thus complemented by minor variations of the B_{NH_3} coverage as a result of adsorption/desorption.

The molecular level information on the vanadium reduction/oxidation present in the phase-resolved DRIFT data was enriched by important details concerning the V=O and V–OH groups involved in this chemistry. The spectra allowed distinguishing between the reactivity of isolated V=O and the NH_3 adsorption capacity of WO_3.[10] Isolated V=O species are expected in VWT because of the sub-monolayer vanadium coverage and the tendency of vanadium to disperse on a WO_3-TiO_2 surface while the existence of adjacent V=O groups is unlikely. However, the signature of the isolated V=O groups at 2045 cm^{-1} was observed only for the sequences depicted in Figure 3 and Figure 4a–c.[17] In all other cases, perturbation of W=O tungstenyl species (2005 cm^{-1}) always masked the contribution of V=O, which is reasonable based on the above observation that NH_3 adsorption/desorption was present in those sequences. The appearance of V=O species simultaneous to L_{NH_3} consumption confirmed that NH_3 dissociated on V=O in the presence of NO, thus producing a V–OH group (3660 cm^{-1}). The V–OH group in turn was oxidized by oxygen and restored to unoccupied V=O (steps (c) and (d) in Scheme 1). This observation is consistent with a concerted transfer of a hydrogen atom to the coordinating vanadium mono-oxo group simultaneous to the formation of the N–N bond of the intermediate (Supporting Information, Figure S9). Moreover, this observation helps to explain the

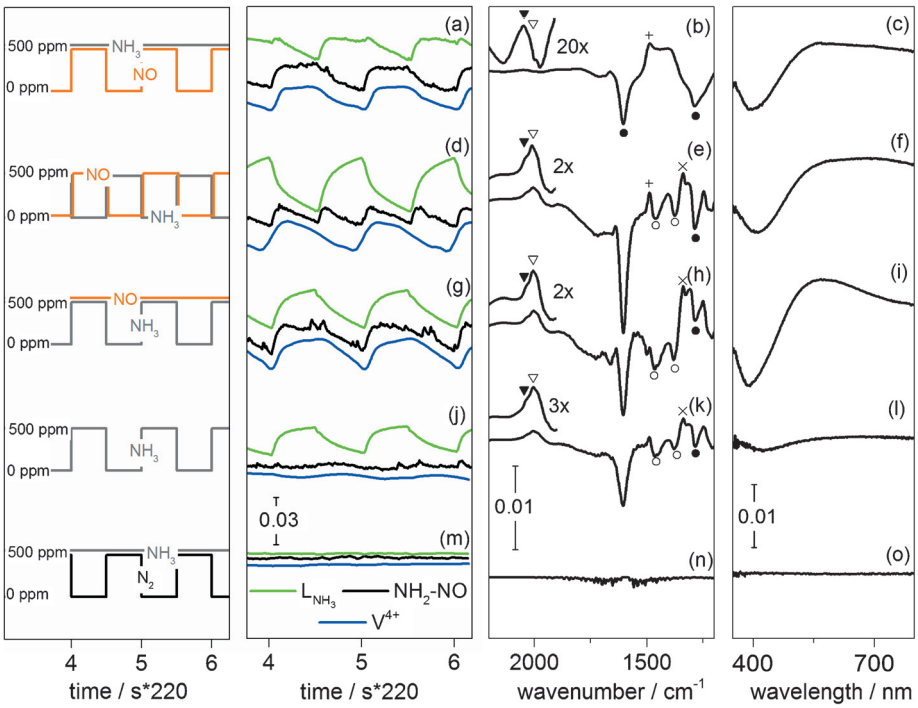

Figure 4. Concentration modulation sequences. Representation of the modulation sequences performed with DRIFTS and DR-Vis ($T = 220$ s): a)–c) NO pulses in NH_3, d)–f) alternated NO and NH_3 pulses, g)–i) NH_3 pulses in NO, j)–l) NH_3 pulses in inert conditions, and m)–o) pulses of N_2 in NH_3. (a, d, g, j, m) NH_2NO and L_{NH_3} peak intensity of the time-resolved DRIFTS spectra and absorbance of V^{4+} of the time-resolved DR-Vis spectra. Corresponding phase-resolved (b, e, h, k, n) DRIFTS and (c, f, i, l, o) DR-Vis data; only the in-phase spectra are displayed. Minimum and maximum NO and NH_3 concentration values are 0 ppm and 500 ppm, respectively. Key: L_{NH_3} (●); NH_2NO (+); B_{NH_3} (○); S=O (×); V=O (▼); W=O (▽). Conditions: pulses of NH_3 (500 ppm) and/or NO (500 ppm); constant O_2 (5 vol%) in N_2; 250 °C.

observed increased V^{5+} reduction only upon reaction of adsorbed NH_3 and gas phase NO. The direct involvement of the V^{4+}/V^{5+} pair in the sequence of NO pulses in NH_3 was disclosed by the phase-resolved data, while virtually no change in the oxidation state of vanadium was visible in time-resolved DR-Vis (Supporting Information, Figure S8). The fraction of vanadium changing repeatedly between V^{5+} (reducing in the presence of both NO and NH_3) and V^{4+} (slowly oxidizing in the subsequent $NH_3 + O_2$ pulse) was clearly visible, in agreement with the transient experiment depicted in Figure 1.

The results show that the two peculiar functions present on a vanadium-based SCR catalyst can be probed by time-resolved spectroscopic methods. To this end, we could clearly separate between reactive sites and NH_3 adsorption/desorption sites.[10] Although we cannot state whether NH_3 adsorbed on Brønsted acid sites desorbs in the gas phase prior to adsorption onto Lewis acid sites, the role of Brønsted acid sites is clearly that of an NH_3 reservoir. The SCR active redox sites are only associated with vanadium Lewis acid sites—likely isolated mono-oxo vanadyl groups.

The combined transient time-resolved DRIFTS and DR-Vis study adds a new perspective to the SCR mechanism over V_2O_5-WO_3-TiO_2, using a time scale pertinent to the observation of active, intermediate, and spectator species. Using tailored time-resolved pulse experiments we were able to describe the entire mechanism of standard NH_3-SCR. NO reacts predominantly with NH_3 adsorbed on Lewis acid sites at low temperature. Despite their abundance, Brønsted acid sites hardly contribute to the SCR activity and mainly serve as an NH_3 pool to replenish the Lewis sites. The active Lewis acid site consists of isolated V^{5+}, which reduces only in the presence of both NO and NH_3. On top of this, we were able to verify the formation of the nitrosamide intermediate, which is formed alongside V^{5+} reduction. Once consumed, the active Lewis sites must be regenerated upon re-oxidation, which is the rate-determining step.

Acknowledgements

The authors kindly acknowledge the financial support of Treibacher Industrie AG and K. Schermanz and A. Deutsch for fruitful discussions. The study has been conducted in the framework of the SCCER BIOSWEET program.

Keywords: Lewis acid sites · mechanisms · modulated excitation · NH_3-SCR · operando spectroscopy

How to cite: *Angew. Chem. Int. Ed.* **2016**, *55*, 11989–11994
Angew. Chem. **2016**, *128*, 12168–12173

[1] a) P. Forzatti, *Appl. Catal. A* **2001**, *222*, 221–236; b) I. Nova, E. Tronconi, *Urea-SCR Technology for DeNOx After Treatment of Diesel Exhausts*, Springer, New York, **2014**.
[2] a) M. Inomata, A. Miyamoto, Y. Murakami, *J. Catal.* **1980**, *62*, 140–148; b) G. Ramis, G. Busca, F. Bregani, P. Forzatti, *Appl. Catal.* **1990**, *64*, 259–278; c) N. Y. Topsøe, *Science* **1994**, *265*, 1217–1219; d) T. V. W. Janssens, H. Falsig, L. F. Lundegaard, P. N. R. Vennestrøm, S. B. Rasmussen, P. G. Moses, F. Giordanino, E. Borfecchia, K. A. Lomachenko, C. Lamberti, S. Bordiga, A. Godiksen, S. Mossin, P. Beato, *ACS Catal.* **2015**, *5*, 2832–2845; e) M. Takagi, T. Kowai, M. Soma, I. Onishi, K. Tamaru, *J. Catal.* **1977**, *50*, 441–446.
[3] M. A. L. Vargas, M. Casanova, A. Trovarelli, G. Busca, *Appl. Catal. B* **2007**, *75*, 303–311.
[4] G. Busca, L. Lietti, G. Ramis, F. Berti, *Appl. Catal. B* **1998**, *18*, 1–36.
[5] a) M. D. Amiridis, R. V. Duevel, I. E. Wachs, *Appl. Catal. B* **1999**, *20*, 111–122; b) D. Nicosia, M. Elsener, O. Kröcher, P. Jansohn, *Top. Catal.* **2007**, *42–43*, 333–336; c) C. Sun, L. Dong, W. Yu, L. Liu, H. Li, F. Gao, L. Dong, Y. Chen, *J. Mol. Catal. A* **2011**, *346*, 29–38.
[6] M. Gruber, K. Hermann, *J. Chem. Phys.* **2013**, *139*, 244701–244708.

[7] L. Lietti, J. L. Alemany, P. Forzatti, G. Busca, G. Ramis, E. Giamello, F. Bregani, *Catal. Today* **1996**, *29*, 143 – 148.
[8] F. Giraud, C. Geantet, N. Guilhaume, S. Loridant, S. Gros, L. Porcheron, M. Kanniche, D. Bianchi, *J. Phys. Chem. C* **2015**, *119*, 15401 – 15413.
[9] N. Y. Topsøe, H. Topsøe, J. A. Dumesic, *J. Catal.* **1995**, *151*, 226 – 240.
[10] L. Lietti, I. Nova, S. Camurri, E. Tronconi, P. Forzatti, *AIChE J.* **1997**, *43*, 2559 – 2570.
[11] a) A. Marberger, M. Elsener, D. Ferri, K. O, *Catalysts* **2015**, *5*, 1704 – 1720; b) G. Madia, M. Elsener, M. Koebel, F. Raimondi, A. Wokaun, *Appl. Catal. B* **2002**, *39*, 181 – 190.
[12] a) A. A. Tsyganenko, D. V. Pozdnyakov, V. N. Filimonov, *J. Mol. Struct.* **1975**, *29*, 299; b) N. Y. Topsøe, *J. Catal.* **1991**, *128*, 499 – 511.
[13] a) A. Brückner, *Chem. Commun.* **2005**, 1761 – 1763; b) L. Burcham, G. Deo, X. Gao, I. E. Wachs, *Top. Catal.* **2000**, *11 – 12*, 85 – 100.
[14] a) M. Koebel, G. Madia, M. Elsener, *Catal. Today* **2002**, *73*, 239 – 247; b) E. Tronconi, I. Nova, C. Ciardelli, D. Chatterjee, M. Weibel, *J. Catal.* **2007**, *245*, 1 – 10.
[15] a) I. E. Wachs, *Catal. Today* **2005**, *100*, 79 – 94; b) I. E. Wachs, *Dalton Trans.* **2013**, *42*, 11762 – 11769; c) G. T. Went, L. J. Leu, R. R. Rosin, A. T. Bell, *J. Catal.* **1992**, *134*, 492 – 505.
[16] a) D. Baurecht, U. P. Fringeli, *Rev. Sci. Instrum.* **2001**, *72*, 3782 – 3792; b) A. Urakawa, T. Bürgi, A. Baiker, *Chem. Eng. Sci.* **2008**, *63*, 4902 – 4909; c) D. Ferri, M. A. Newton, M. DiMichiel, G. L. Chiarello, S. Yoon, Y. Lu, J. Andrieux, *Angew. Chem. Int. Ed.* **2014**, *53*, 8890 – 8894; *Angew. Chem.* **2014**, *126*, 9036 – 9040.
[17] G. Busca, G. Centi, L. Marchetti, F. Trifirò, *Langmuir* **1986**, *2*, 568 – 577.

Received: June 2, 2016
Revised: July 18, 2016
Published online: August 24, 2016

